M. Thomsen, C. Fernandez-Pello, X. Huang, S. Olson, P. Ferkul (2019) Opposed Flow Burning of PMMA Cylinders in Normoxic Conditions, Fire Safety Journal, 110, 102903. https://doi.org/10.1016/j.firesaf.2019.102903
This is the Pre-Published Version.

Opposed Flow Burning of PMMA Cylinders in Normoxic Atmospheres

MARIA THOMSEN[1], CARLOS FERNANDEZ-PELLO[1], XINYAN HUANG[2], SANDRA L. OLSON[3] and PAUL V. FERKUL[3]
[1]Department of Mechanical Engineering
University of California, Berkeley
Berkeley, CA, 94720, USA
[2]Department of Building Services Engineering,
The Hong Kong Polytechnic University, Hung Hom, Kowloon, Hong Kong
[3]NASA John H. Glenn Research Center
Cleveland, OH, 44135, USA

ABSTRACT

The influence of environmental conditions on the flammability of combustible solids is of importance to spacecraft fire safety because of the differences with the conditions encountered on Earth. In a manned spacecraft there is reduced gravity and low velocity flows. Additionally, the environment is maintained at Normoxic conditions, which is the combination of ambient pressure and oxygen concentration that results in a partial pressure of oxygen equal to that of normal atmosphere at sea level ($P_{O_2} = 21kPa$). Future spacecraft will have atmospheres with reduced pressures and oxygen concentrations at Normoxic conditions (Space Exploration Atmospheres - SEA), designed to reduce preparation time for spacewalks. This work studies the effect of ambient pressure and oxygen concentration, on opposed flame spread and mass burning in cylindrical samples of polymethyl methacrylate (PMMA). Experiments in normal gravity are conducted using ambient pressures ranging between 100 and 60 kPa and oxygen concentrations between 21% and 35% by volume, while maintaining Normoxic conditions. Results show that moving to Normoxic environments with reduced pressure and increased oxygen concentration increases the flammability of the PMMA cylinders. The data presented here provide information about the flammability of spacecraft materials in future SEA, yielding insight for future designs when considering fire safety in spacecrafts.

KEYWORDS: Flame spread; surface burning; Normoxic conditions; PMMA

1. INTRODUCTION

Fire safety in spacecraft environments is an important concern for space travel [1,2] particularly because of the criticality of such an event. Inside a spacecraft cabin or a space facility there are combustible materials, and conditions that can be favorable for ignition, thus posing the risk of initiating a fire. Also, the enclosed nature of space facilities, where egress is difficult or almost impossible, means that the consequences of a fire could be catastrophic for the crew's safety. The fire risk associated with these environments will increase as the time spent in space is increased with the operation of proposed long space missions, and the establishment of facilities on the Moon and Mars. Consequently, understanding solid material flammability in the environments expected in space facilities is of importance to better characterize the fire risk. Flammability of a material is typically characterized by its ease of ignition, flame spread rate, heat release rate, and toxicity [3]. The most effective fire safety strategy is to prevent ignition. However, following ignition, flame spread presents a significant safety risk to space travel. Thus, experiments on flame spread are often used to determine the fire hazard of a material and the corresponding fire-extinguishing strategy [4].

A problem with testing on Earth the flammability of materials to be used in space facilities is that spacecraft/space facilities ambient conditions are very different from those encountered on Earth since they include microgravity, or reduced gravity, low velocity flows, and potentially low pressure and elevated oxygen concentration, while maintaining Normoxic conditions in manned spacecraft [5]. These atmospheric conditions are referred to as Space Exploration Atmospheres (SEA) and are designed to reduce the preparation time required before Extra Vehicular Activities (EVA) while keeping the partial pressure of oxygen acceptable for human respiration (Normoxic conditions) [5]. However, because of these new

environmental conditions, material flammability may be affected, resulting in an even higher fire risk. So far, because of the restrictions inside of a spacecraft and the very few opportunities available, most of the microgravity testing has focused on normal or lower oxygen concentrations and standard ambient pressure and has addressed the limiting conditions for burning [6–8]. There have been a few studies focusing on environments with higher oxygen concentrations, however most of them focused only in thermally thin samples [9–12] and do not include reduced ambient pressure. Other researchers have devoted some efforts to study the effect of these types of environments on piloted ignition [13], spread rate [10,14,15], flammability boundaries [16–18], among others.

The new SEA cabin environments planned by NASA will not only affect the spreading of the flames over a solid fuel surface, but they will also influence the burning of the solid fuel behind the flame front. These two processes, flame spread and mass burning, although different, are coupled through energy and mass balances during the spread of the flame. The spread of the flame is a surface process where the flame transfers heat to the unburnt solid ahead of the pyrolysis region, heating and pyrolyzing it, and subsequently igniting the pyrolyzate, which continues the spread of the flame. In the case of opposed flame spread, the gas flow and the flame spread are in opposite directions. The flame heats and pyrolyzes the solid upstream of the pyrolysis front, which subsequently mixes with incoming oxidizer to form a flammable gas mixture that is then ignited by the flame. Thus, flame spread can de described as a creeping process where the flame acts both as a source of heat to pyrolyze the fuel, and a pilot to ignite the flammable mixture ahead of the flame front. The flame basically consists of a premixed flame that anchors a diffusion flame downstream of the pyrolysis front. The solid burning behind the flame front is a process where the established diffusion flame transfers heat to the already pyrolyzing solid continuing its pyrolysis and burning. The solid pyrolysis and resulting mass loss cause the solid burning surface to regress at a rate that depends on the environmental conditions. The combination of the flame spread rate and regression rate forms an inclined surface downstream of the pyrolysis front, whose angle depends on the relative value of the flame spread rate and regression rate (Fig. 1).

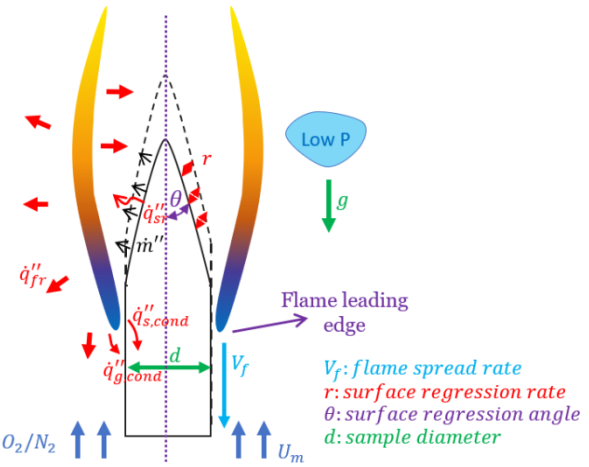

Fig. 1. Schematic representation of the rod burning process.

Some previous studies have analyzed the relation between flame spread and fuel regression behind the flame. Burning rate has been measured and described through theoretical models using boundary layer approximations [19–23]. These studies determined that the burning rate was proportional to the B number and the Grashof number or Reynolds number, depending on whether free or forced convection was considered. Sibulkin and coworkers [24,25] studying the downward burning of PMMA cylinders observed that the cylinder would form a cone behind the pyrolysis front, the angle of which would increase as the oxygen concentration was reduced. The researchers also noticed that the flame spread was directly proportional to changes in the oxygen concentration; however, those changes were not observed in the surface regression rate. Carmignani et al. [26] have also studied the angle generated when flames spread downward over flat PMMA samples. They observed that the angle would be a function of material thickness and it would be related to the burning rate. They also showed that, for thermally thick solids, the angle eventually reaches an asymptotic value. Huang et al. [27] showed that, depending on the environmental conditions,

either a flame spread dominated regime or a mass burning dominated regime would characterize the opposed/downward burning of PMMA rods. The transition between the two regimes could be related to the burning angle formed. The results of these works suggest that in opposed flame spread there is an intrinsic relation between flame spread and surface regression, that is strongly influenced by the environment in which the solid fuel is burning. In fact, there are questions regarding whether what is usually referred as flame spread is actually flame spread or surface regression [27]. Currently, there is insufficient understanding of the relation between these two processes, not to mention their role in environments similar to those expected in future spacecraft. Thus, further research is needed to better understand how these new spacecraft environments will affect material flammability.

This work presents experiments conducted to study the effect of Normoxic ambient pressure and oxygen concentration in the burning behavior of PMMA rods in an opposing gas flow in normal gravity. A normoxic environment is considered as the combination of ambient pressure and oxygen concentration that results in a partial pressure of oxygen equal to that of normal atmosphere at sea level ($P_{O_2} = 21kPa$). The tests are conducted with the cylindrical samples positioned vertically, such that the gravity vector is parallel to the sample centerline and the forced gas flow moves upward, such that the flame spreads downward in an opposed mixed (free and forced) gas flow. A few tests conducted in microgravity in the International Space Station (ISS) are also compared with the normal gravity tests to infer the effect of microgravity on the flame spread process.

2. EXPERIMENT DESCRIPTION

Normal gravity experiments were conducted in an apparatus previously developed to study the flammability of solid combustible materials under varied ambient conditions [18]. The apparatus consists of a laboratory scale combustion tunnel that has a 125 mm by 125 mm cross section and is 600 mm in length. The first section of the duct serves as a flow straightener while the other segment of the duct is used as the test section. The tunnel is inserted in a 105 L pressure chamber as shown in Fig. 2. The chamber has a flow system that provides constant supply and exhaust of gases to keep the pressure constant and to avoid vitiation problems. Compressed house air or nitrogen and oxygen are supplied through critical nozzles (O'Keefe Controls) to the bottom of the duct while at the same time evacuating to maintain constant pressure inside the chamber. The chamber pressure is controlled by a high-capacity vacuum generator (Vaccon JS-300) and a mechanical vacuum regulator. The chamber pressure is monitored continuously with an electronic pressure transducer (Omega Engineering, Inc. PX303-015A5V). The tests were conducted at Normoxic conditions with pressures ranging between 100 and 60 ± 2 kPa, and oxygen concentrations determined by the corresponding Normoxic value. The forced flow velocity was fixed to 100 mm/s in all the tests, a value which is similar to that induced by the HVAC in spacecraft.

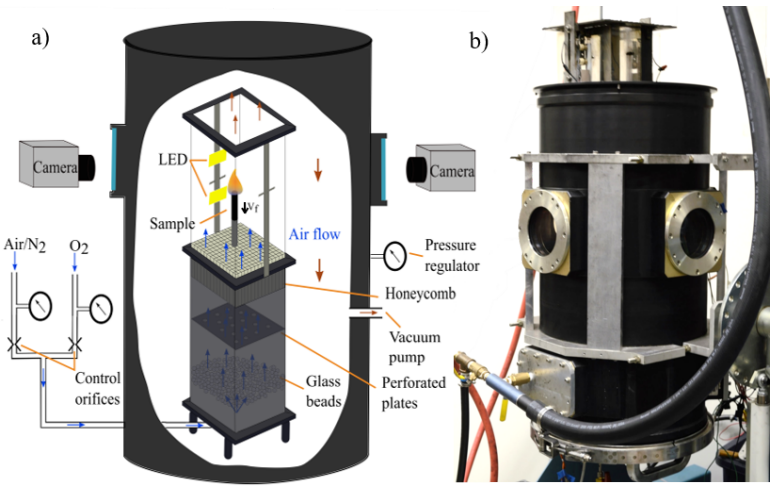

Fig. 2. (a) Schematic of experimental apparatus and (b) normal gravity experimental setup.

The sample was placed vertically in the center of the test section, supported on a metal cylinder of the same diameter to prevent flow disturbances. Sample ignition was induced with a 26-gage Nichrome wire coil on top of the upstream edge of the sample under normal ambient pressure as shown in Fig. 3. The igniter was energized using a variable transformer (STACO Energy model 3PN1210B). Once the sample was in position and ignition was achieved, the chamber was sealed to adjust the system to the desired conditions. Two 9000 lumen LED were installed with an operating electronic circuit to act as a strobe light to visualize the pyrolysis region and measure flame spread rates, surface regression rates, and cone angle, and to observe the flame appearance. Each test was video recorded with two different cameras: a Nikon D3200 with a resolution of 1280 by 720 at 59 frames per second and a Sony RX10-III with a resolution of 1920 by 1080 at 120 frames per second. For each test condition, at least 5 experiments were conducted to address the experimental uncertainty.

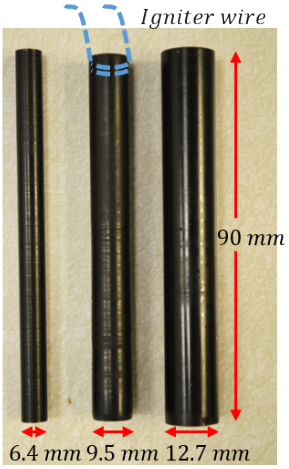

Fig. 3. PMMA samples tested.

The samples used in the experiments were made of cast black polymethyl methacrylate (PMMA). Sample length was 90 mm and sample diameters were 12.7, 9.5, and 6.4 mm (Fig. 3). The sample material and geometry were selected following previous experiments conducted in the ISS under the BASS-II project [7]. In addition, PMMA is typical of non-charring thermoplastics and has been widely used in the past because of its well determined properties. Furthermore, PMMA is potentially going to be used in some components, such as windows, in future spacecrafts.

3. RESULTS

Opposed flame spread over the surface of the PMMA rods was investigated under different Normoxic environments by using reduced ambient pressure and increased oxygen concentration combinations. The primary data collected from the video recordings was the flame spread rate, surface regression rate and the surface regression angle (Fig. 1). Once ignition was obtained, the flame was observed as it propagated downward over the sample. The rate of flame spread was determined by tracking the position of the leading edge of the flame with time. Regression rate was measured by tracking the position of the PMMA surface. The regression angle was measured at the end of the spread to get a value as close to the steady state as possible. The rate of spread of the flame was observed to approach steady state soon after the sample was ignited (~ 1 min). The mass loss rate, however, took longer to reach steady state and the time was dependent on the environmental conditions tested. For example, for the 21% O_2 and 100 kPa conditions it took about 3 min for the regression rate to reach steady state, while for the 35% O_2 and 60 kPa steady state was not reached after the flame spread over the whole sample and the experiment terminated.

Figure 4 shows still frames from videos taken in normal gravity with various Normoxic environments, with ambient pressure ranging from 100 to 60 kPa and oxygen concentration increasing from 21% to 35%. As the ambient pressure is reduced and the oxygen concentration is increased the flame gets longer and brighter. At higher oxygen concentrations, significant vapor jetting of bubbles of PMMA bursting at the surface are also observed, causing distortions in the flame as the test progresses [28].

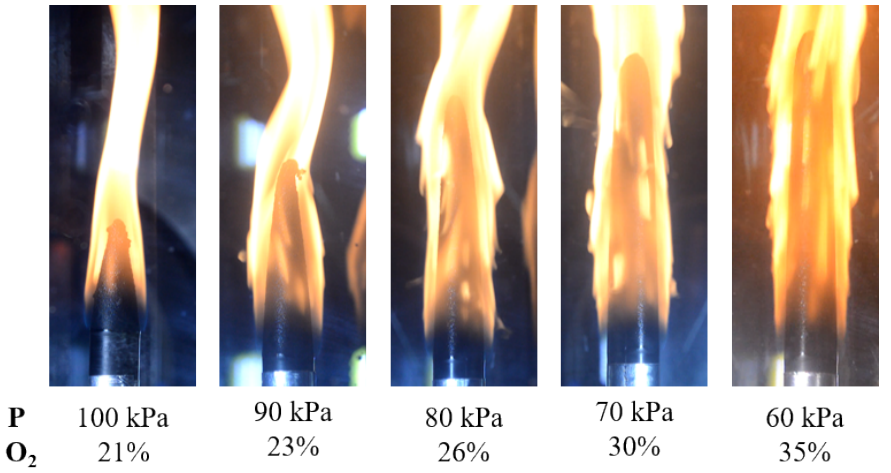

Fig. 4. Photo sequence of normal gravity flame appearance in Normoxic environments with different ambient pressure and oxygen concentration. Sample diameter was 12.7 mm.

Figure 5 shows the progress of the leading edge of the flame as it propagates over the PMMA surface for representative tests in the same Normoxic environments presented in Fig. 4. From the figure, it is seen that the flame spread is fairly steady over time. It is also seen that, as the pressure is reduced and oxygen concentration is increased, the spread of the flame is faster.

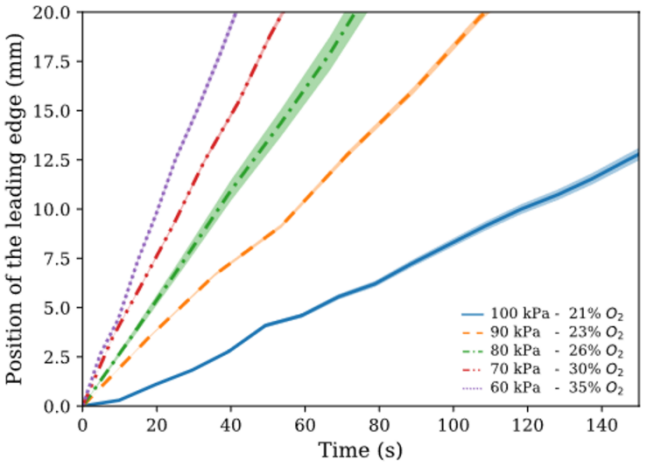

Fig. 5. Position of the leading edge of the flame as a function of time in different Normoxic environments. Sample diameter was 12.7 mm.

The progress of the flame's leading edge can be used to determine the flame spread rate. Figure 6 shows the average flame spread rate as a function of ambient pressure as obtained from the data of Fig. 5. Error bars are included and calculated from the standard deviation among tests done at similar conditions. The downward flame spread process was steady and uniform, and the highest standard deviation between comparable tests was negligible (error below 5.4%). It is seen from Fig. 6 that, as environments are changed to reduced ambient pressure and increased oxygen concentration, the rate of spread of the flame over the solid surface increases. Since at constant oxygen concentration the spread rate decreases with pressure [29], this indicates that, in Normoxic atmospheres, the changes in oxygen concentration have a stronger effect than the changes in pressure, and that there is an increase in material flammability at Normoxic conditions with higher oxygen concentrations. Also, it is seen that as the diameter of the sample is reduced the opposed flow flame spread rate increases. This is due to the faster heating of the thinner samples and to the heat transfer from the flame to the solid being enhanced by the increase in the curvature of the surface [30]. The observed dependence of the spread rate on the rod diameter indicates that the samples tested are not thermally thick. This is enhanced as the oxygen concentration is increased and the pressure reduced. Data obtained during the BASS-II experiments [29], at similar conditions of oxygen and pressure, have also been included in Fig. 6

for comparison purposes. Form the figure it is seen that, at least at 100 kPa in normal air, in microgravity the flame spread is smaller than in normal gravity, with the flame spread rate also increasing for decreasing sample diameters.

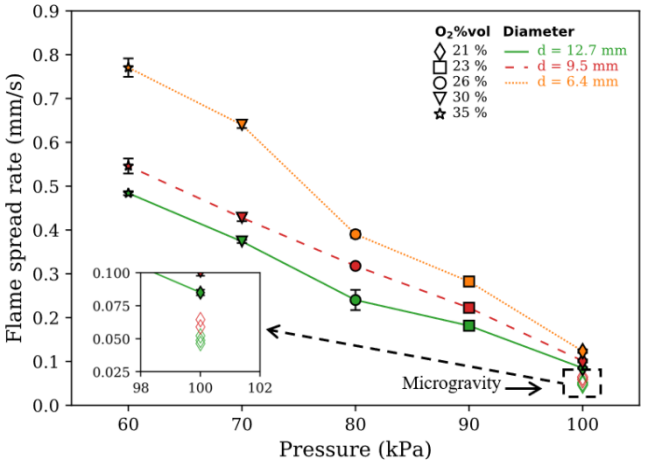

Fig. 6. Flame spread rate as a function of ambient pressure in different Normoxic environments. Microgravity data obtained from BASS-II experiments [29] at similar conditions are included with empty markers.

Figure 7 shows the data presented in Fig. 6 but as a function of the sample diameter. It is seen from the figure that the dependence of the flame spread rate on the sample diameter changes depending on the environmental conditions. For 100 kPa and 21% O_2 the flame spread rate is almost independent of the sample radius, indicating that the rods behave as thermally thick solids [31]. However, the thickness dependence changes for the lower pressure Normoxic environments such as 60 kPa and 35% O_2, where a dependence of the radius on $r^{-0.69}$ is found, closer to the r^{-1} observed with thermally thin solids [31]. Thus, the cylinders used in this work appear to transition from a thermally thick to a thermally thin solid type of flame spread as the pressure is decreased and the oxygen concentration increased.

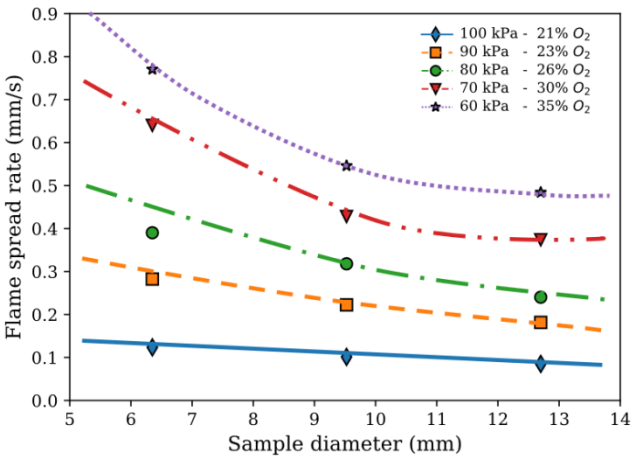

Fig. 7. Flame spread rate as a function of the sample diameter.

Along with flame spread rate, the surface regression rate was also measured. The results are presented in Fig. 8 for the three sample diameters tested. Error bars in these figures are also obtained from the standard deviation between comparable tests. From Fig. 8 it can be noted that, as ambient pressure is reduced and oxygen concentration is increased, the regression rate decreases with pressure but becomes almost constant for pressures lower than 80 kPa. The dependence at lower pressures appears to be the result of the surface regression rate not achieving steady state at oxygen concentrations larger than 26% due to the faster spread of the flame reaching the end of the sample before the regression rate reaches steady state. It is seen that the

flame spread rate and regression rate have opposite dependences on pressure, or oxygen concentration, at Normoxic conditions. This is somewhat surprising since the heat transfer mechanisms, particularly the heat transfer from flame to fuel, are similar for flame spread and regression rate. Also interesting is that the sensitivity of the spread rate to changes in oxygen concentration is significantly higher than that of the surface regression rate, in agreement with the observations of Sibulkin and Little [25].

The regression angle is obtained either from the ratio of the flame spread rate and regression rate, or directly from the videos of the flame spread. From the results presented in Fig. 9 it is seen that the regression angle decreases as the ambient pressure is decreased and the oxygen concentration is increased in Normoxic conditions. Although the decreasing trend with pressure seems to follow that of the regression rate, the dependence of the regression angle with pressure is more sensitive to environmental changes than the regression rate. This seems to be due to the strong variation of the flame spread rate along the Normoxic pressure and oxygen conditions. Also, the angle of the cone is almost independent of the diameter of the sample.

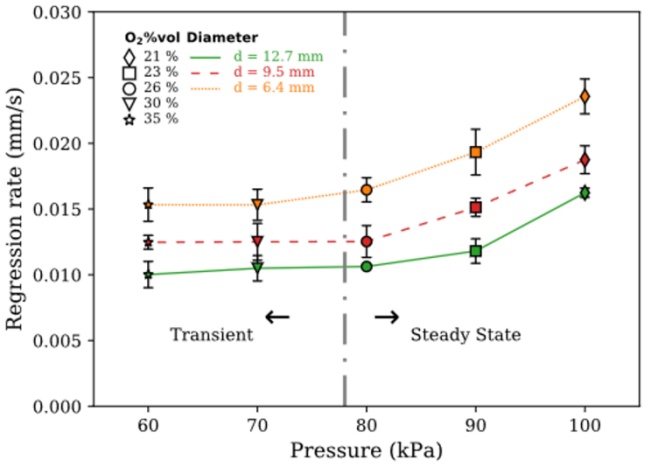

Fig. 8. Surface regression rate as a function of ambient pressure in different Normoxic environments.

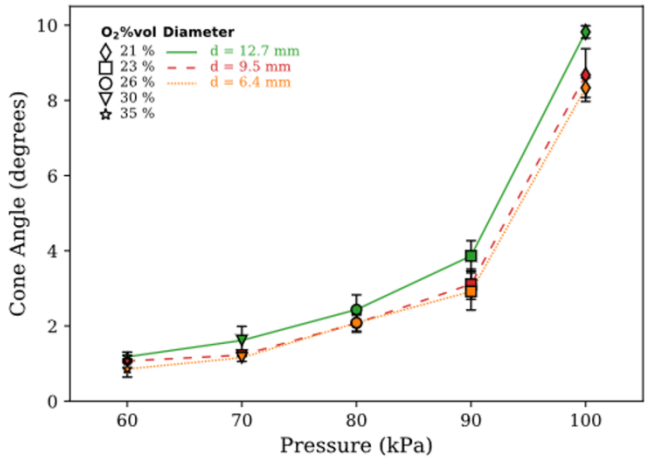

Fig. 9. Cone angle as a function of ambient pressure in different Normoxic environments.

4. DISCUSSION

The behavior of opposed flow flame spread is the result of a complex process controlled by the interaction between the solid phase (heat transfer, thermal decomposition, gasification) and the gas phase (transport, mixing, chemical kinetics) [31–34]. As the flame propagates it heats up the solid fuel ahead from its initial temperature to its pyrolysis temperature, and then pyrolyzes it. The pyrolyzate mixes with the ambient

oxidizer forming a flammable mixture that is ignited by the flame causing it to propagate along the solid surface. Because of the complexity of the problem, analytical models of flame spread have been traditionally divided into two subcategories, thermally thick or thin solids [35]. Thermally thick solids are characterized by having a varying temperature profile along their cross section that does not penetrated the whole solid thickness, whereas in thermally thin solids the temperature profile across the thickness of the fuel is uniform. The characteristics of the solid temperature profile depend on the problem parameters (solid thermal properties and surface heat flux), thus a solid may behave as thermally thin or thick regardless of its physical thickness. In most practical cases the solid is not either thin or thick.

Several theoretical models have been developed [30–32,36–38], following the thermally thick and thin classification. Despite of the simplification these theoretical models provide a useful tool to understand from a phenomenological point of view how the variables of interest influence the rate of spread of the flame for both, thermally thin and thermally thick solids. The analysis developed by Delichatsios [30] for a cylindrical geometry provides analytical expressions for the opposed flame spread rate over a solid rod for a thermally thin solid as:

$$V_f = 2f_{cyl}\left(\frac{k_g}{\rho_s c_s r}\right)\left(\frac{T_f - T_p}{T_p - T_\infty}\right) \tag{1}$$

and for a thermally thick solid as:

$$V_f = f_{cyl}\left(1 - \frac{k_s(T_p - T_\infty)}{\rho_g c_g U_\infty 2r(T_f - T_p)}\right)^{-1}\left(\frac{k_g \rho_g c_g}{k_s \rho_s c_s}\right)\left(\frac{T_f - T_p}{T_p - T_\infty}\right)^2 U_\infty \tag{2}$$

where f_{cyl} is a geometrical factor that accounts for the curvature effect of the surface and is defined as

$$f_{cyl} = c(L_g/r)/ln\left(1 + \frac{cL_g}{r}\right) \tag{3}$$

In the equations V_f is the flame spread rate and U_∞ is the air flow velocity. ρ_s, k_s and c_s are the solid density, thermal conductivity and specific heat. ρ_g and $c_{p,g}$ are the gas density and specific heat, and k_g is the gas thermal conductivity. T_f, T_p and T_∞ represent the flame, pyrolysis and ambient temperature, respectively. L_g is the diffusion length, c is a numerical constant, and r is the cylinder radius. It should be mentioned that Eq. (1) and (2) describe the spread of flames in the thermal regime, and thus they do not include the influence of any chemical kinetics effects. Nevertheless, these equations are still applicable at the ambient conditions in this work, i.e. elevated oxygen concentrations and ambient pressures not lower than 60 kPa, where chemical kinetics are not expected to be dominant [13]. The primary predictions of the analysis are that for thermally thin rods the flame spread is inversely proportional to the rod radius and independent of the flow velocity. For thermally thick cylinders the flame spread rate is weakly dependent on the rod radius, and proportional to the gas flow velocity.

From the experimental results presented in Fig. 6 it appears that the rods tested behave between thermally thick and thin, depending on the ambient conditions, since the flame spread rate depends on the rod radius but not inversely proportional to the radius. Furthermore, since Eqs. (1) and (2) predict a different dependence on the gas flow velocity for thin or thick solids, it is of interest to plot the experimental data in terms of the flow velocity U_∞. In the present experiments the gas flow is mixed, free and forced, and the free (buoyant) flow velocity depends on the environmental conditions, thus U_∞ is defined as

$$U_\infty = U_f + U_b = U_f + (gL_c\Delta\rho_g/\rho_g)^{1/2} \tag{4}$$

where g is gravity and L_c is the characteristic buoyant length, and $\Delta\rho_g$ is $\rho_g - \rho_a$. Determining L_c is complex since it should depend on the flow and sample configuration, so for simplification purposes in the present work it is assumed to be a constant value. From Eq. (4) it is seen that the mixed flow velocity to which the flame is exposed changes as a function of oxygen and pressure through changes in the gas phase density due to changes in the flame temperature. For the purpose of the analysis, the flame temperature was considered as the adiabatic flame temperature at each condition.

Figure 10 presents the flame spread data of Fig. 6 as a function of the mixed flow velocity, U_∞ for the three rods and Normoxic conditions tested. From Fig. 10 it is seen that the flame spread depends linearly on the flow velocity for all the rods tested. This is an interesting result since, according to Eq. (2), the dependence on the flow velocity of the flame spread rate shown in Fig. 10 would indicate that the rod samples are behaving as a thermally thick solid. However, the results of Fig. 7 indicate that the samples do not behave as thermally thick since the spread rate depends on the sample diameter. Furthermore, both the results from Fig. 7 and Fig. 10, together with Eqs. (1) and (2) suggest that the characteristics of the flame spread rate may transition from those of a near thermally thick solid toward a thermally thin one as the Normoxic conditions are changed to lower pressures and higher oxygen concentrations. This behavior between the two regimes poses a challenge particularly when trying to use simplified analytical models to predict flame spread behavior over practical materials.

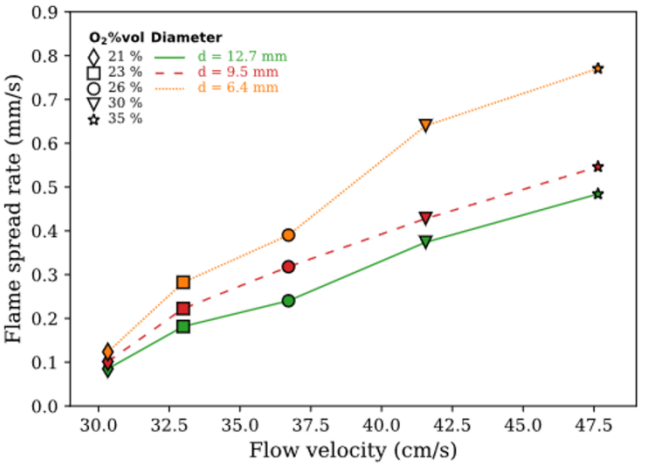

Fig. 10. Flame spread rate as a function of the mixed flow velocity in different Normoxic environments.

The present results provide a phenomenological interpretation of the flame spread in the present experiments. Analyzing the solid heating by the flame when the Normoxic conditions change, as the oxygen concentration increases the flame temperature increases and so does the heat flux from the flame to the solid. Consequently, the flame spread rate increases as observed in the experiments (Fig. 6). However, as the flame spreads faster a thinner layer of the solid fuel is been heated up. This causes the material to behave as a thermally thick solid since, in practice, only a thin layer of the solid is being heated. Thus, the spread rate should be independent of the rod radius, contrary to the present results. Similar arguments can be made as the mixed flow velocity is increased. Thus, it appears that the simplification of classifying a solid combustible as thermally thick or thermally thin for the purpose of predicting opposed flow flame spread may be limited only to some environmental conditions, but it might not work to predict the variation of the spread rate at different Normoxic environments.

Figure 11 presents the regression rate experimental data of Fig. 8 as a function of the mixed flow velocity U_∞. It is seen that the surface regression rate depends on the mixed flow velocity for all the rods tested, decreasing as the flow velocity is increased, at least for the steady state conditions. This result is surprising since as the flow velocity is increased the flame moves closer to the solid surface, and consequently the heat flux from the flame to the solid should increases, which should result in an increase of the regression rate. It is also surprising that the regression rate decreases in Normoxic environments with higher oxygen concentrations, since the flame temperature should increase, and in turn the heat flux on the surface. At the higher oxygen concentration, the spread of the flame becomes faster (reducing the characteristic time of the process), and the time for heat to penetrate into the solid is reduced. Consequently, the surface regression rate is reduced, and it may reach the point that steady state is not achieved within the length of the samples tested.

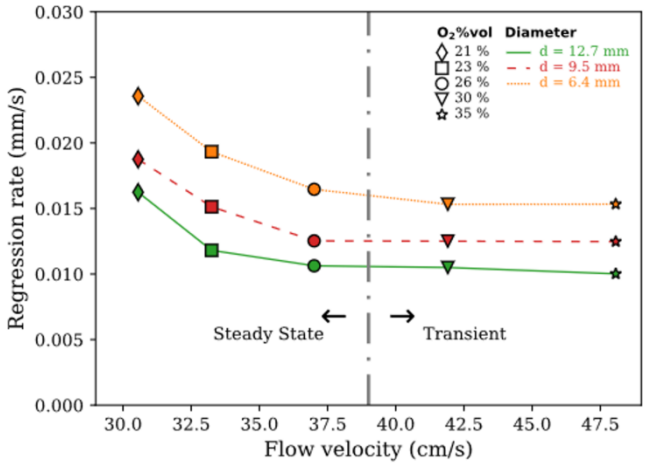

Fig. 11. Surface regression rate as a function of flow velocity in different Normoxic environments.

5. CONCLUSIONS

This work has studied the opposed flame spread and fuel regression of black cylindrical PMMA samples of different diameters under different Normoxic environments (with reduced ambient pressure and increased oxygen concentration) following NASA's interest for future space exploration vehicles. The flame spread rate is found to increase in Normoxic environments with elevated oxygen concentration, and with the mixed convection flow velocity that the flame is exposed to. The surface regression rate shows a decreasing trend in Normoxic environments with higher oxygen concentration and mixed flow velocities. It is also found that the dependence of the flame spread rate on the rod diameter depends on the environment conditions, with a transition to a stronger dependence as the Normoxic conditions are changed to lower pressures and higher oxygen concentrations. Similarly, the observation that the surface regression rate decreases as the Normoxic conditions are changed to lower pressure and oxygen concentration appears to contradict phenomenological arguments of the process, indicating that caution should be taken when applying simplified analyses of flame spread and surface regression to spacecraft environments.

Also, worth noting is that the current tests suggest that as spacecraft cabin environments are changed to include reduced cabin pressure and increased oxygen concentrations (Normoxic environments) an increased in the fire risk could occur from the higher flammability of combustible materials at those conditions.

ACKNOWLEDGEMENTS

This work was supported by NASA Grants NNX10AE01G and NNX13AL10A. The authors would like to acknowledge the assistance of Grace Mendoza, Madison Hales, Runbiao Wei, Ryan So, Christina Liveretou, and Andy Rodriguez with the experiments.

REFERENCES

[1] R. Friedman, Fire Safety in Spacecraft, Fire Mater. 20 (1996) 235–243.

[2] G. Jomaas, J.L. Torero, C. Eigenbrod, J. Niehaus, S.L. Olson, P. V Ferkul, G. Legros, A.C. Fernandez-Pello, A.J. Cowlard, S. Rouvreau, N. Smirnov, O. Fujita, J.S. T'ien, G.A. Ruff, D.L. Urban, Fire safety in space – beyond flammability testing of small samples, Acta Astronaut. 109 (2015) 208–216. doi:10.1016/j.actaastro.2014.11.025.

[3] C.W. Lautenberger, J.L. Torero, C. Fernandez-Pello, Understanding materials flammability, in: V.B. Apte (Ed.), Flammabl. Test. Mater. Used Constr. Transp. Min., Woodhead Publishing in Materials, 2006: pp. 1–21.

[4] J.G. Quintiere, Fundamental of Fire Phenomena, John Wiley, New York, 2006.

[5] K.E. Lange, A.T. Perka, B.E. Duffield, F.F. Jeng, Bounding the Spacecraft Atmosphere Design Space for Future Exploration Missions, 2005. http://ntrs.nasa.gov/search.jsp?R=20050185597.

[6] D.L. Urban, P. Ferkul, S. Olson, G.A. Ruff, J.S. T'ien, Y.T. Liao, A.C. Fernandez-Pello, J.L. Torero, G. Legros, C. Eigenbrod, N. Smirnov, O. Fujita, S. Rouvreau, B. Toth, G. Jomaas, Flame Spread : Effects of Microgravity and Scale, Combust. Flame. 199 (2019) 168–182. doi:10.1016/j.combustflame.2018.10.012.

[7] S. Link, X. Huang, C. Fernandez-Pello, S. Olson, P. Ferkul, The Effect of Gravity on Flame Spread over PMMA Cylinders, Sci. Rep. 8 (2018) 120. doi:10.1038/s41598-017-18398-4.

[8] S.L. Olson, P. V. Ferkul, Microgravity flammability boundary for PMMA rods in axial stagnation flow: Experimental results and energy balance analyses, Combust. Flame. 180 (2017) 217–229. doi:10.1016/j.combustflame.2017.03.001.

[9] S. Takahashi, Y. Seki, T. Ihara, K. Wakai, S. Bhattacharjee, Effect of Sample Width on Flame Spread Rate over a Thin Material in Microgravity, Trans. Japan Soc. Aeronaut. Sp. Sci. Sp. Technol. Japan. 7 (2009) 61–66. doi:10.2322/tstj.7.Ph_61.

[10] S.L. Olson, F.J. Miller, Experimental comparison of opposed and concurrent flame spread in a forced convective microgravity environment, Proc. Combust. Inst. 32 (2009) 2445–2452. doi:10.1016/j.proci.2008.05.081.

[11] M. Kikuchi, O. Fujita, K. Ito, A. Sato, T. Sakuraya, Experimental study on flame spread over wire insulation in microgravity, Symp. Combust. 27 (1998) 2507–2514. doi:10.1016/S0082-0784(98)80102-1.

[12] S. Takahashi, H. Ito, Y. Nakamura, O. Fujita, Extinction limits of spreading flames over wires in microgravity, Combust. Flame. 160 (2013) 1900–1902. doi:10.1016/j.combustflame.2013.03.029.

[13] S. McAllister, C. Fernandez-Pello, D. Urban, G. Ruff, The combined effect of pressure and oxygen concentration on piloted ignition of a solid combustible, Combust. Flame. 157 (2010) 1753–1759. doi:10.1016/j.combustflame.2010.02.022.

[14] S.L. Olson, D.W. Griffin, D.L. Urban, G.A. Ruff, E.A. Smith, Flammability of Human Hair in Exploration Atmospheres, SAE Int. J. Aerosp. 4 (2009) 1–6. doi:10.4271/2009-01-2512.

[15] F. Miller, S.L. Olson, I.S. Wichman, A Study of the Effectiveness of a Narrow Channel Apparatus in Simulating Microgravity Flame Spread over Thin Fuels, in: 42nd Int. Conf. Environ. Syst., 2012: pp. 1–8. doi:10.2514/6.2012-3493.

[16] D. Hirsch, J.H. Williams, H. Beeson, Pressure effects on oxygen concentration flammability thresholds of polymeric materials for aerospace applications, J. Test. Eval. 36 (2008) 69–72. doi:10.1520/jte100975.

[17] A.F. Osorio, A.C. Fernandez-Pello, D.L. Urban, G.A. Ruff, Low-pressure flame spread limits of fire resistant fabrics, in: 43rd Int. Conf. Environ. Syst., Vail, CO, 2013: pp. 1–9. doi:10.2514/6.2013-3386.

[18] M. Thomsen, D.C. Murphy, C. Fernandez-Pello, D.L. Urban, G.A. Ruff, Flame spread limits (LOC) of fire resistant fabrics, Fire Saf. J. 91 (2017) 259–265. doi:10.1016/j.firesaf.2017.03.072.

[19] H.W. Emmons, The Film Combustion of Liquid Fuel, J. Appl. Math. Mech. 36 (1956) 60–71. doi:10.1002/zamm.19560360105.

[20] J.S. Kim, J.N. de Ris, F. William Kroesser, Laminar free-convective burning of fuel surfaces, Symp. Combust. 13 (1971) 949–961. doi:10.1016/S0082-0784(71)80095-4.

[21] F.J. Kosdon, F.A. Williams, C. Buman, Combustion of vertical cellulosic cylinders in air, Symp. Combust. 12 (1969) 253–264. doi:10.1016/S0082-0784(69)80408-X.

[22] Y. Pizzo, J.L. Consalvi, P. Querre, M. Coutin, L. Audouin, B. Porterie, J.L. Torero, Experimental

observations on the steady-state burning rate of a vertically oriented PMMA slab, Combust. Flame. 152 (2008) 451–460. doi:10.1016/j.combustflame.2007.06.020.

[23] A.C. Fernandez-Pello, An analysis of the forced convective burning of a combustible particle, Combust. Sci. Technol. 28 (1982) 305–313. doi:10.1080/00102208208952562.

[24] M. Sibulkin, C.K. Lee, Flame Propagation Measurements and Energy Feedback Analysis for Burning Cylinders, Combust. Sci. Technol. 9 (1974) 137–147. doi:10.1080/00102207408960349.

[25] M. Sibulkin, M.W. Little, Propagation and extinction of downward burning fires, Combust. Flame. 31 (1978) 197–208. doi:10.1016/0010-2180(78)90129-3.

[26] L. Carmignani, B. Rhoades, S. Bhattacharjee, Correlation of Burning Rate with Spread Rate for Downward Flame Spread Over PMMA, Fire Technol. 54 (2018) 613–624. doi:10.1007/s10694-017-0698-3.

[27] X. Huang, S. Link, A. Rodriguez, M. Thomsen, S. Olson, P. Ferkul, C. Fernandez-Pello, Transition from opposed flame spread to fuel regression and blow off : Effect of flow, atmosphere, and microgravity, Proc. Combust. Inst. 37 (2019) 4117–4126. doi:10.1016/j.proci.2018.06.022.

[28] M. Thomsen, X. Huang, C. Fernandez-Pello, D.L. Urban, G.A. Ruff, Concurrent flame spread over externally heated Nomex under mixed convection flow, Proc. Combust. Inst. 37 (2019) 3801–3808. doi:10.1016/j.proci.2018.05.055.

[29] M. Thomsen, C. Fernandez-Pello, X. Huang, S. Olson, P. Ferkul, Buoyancy Effect on Downward Flame Spread Over PMMA Cylinders, Fire Technol. (2019) 1–23. doi:10.1007/s10694-019-00866-0.

[30] M.A. Delichatsios, R.A. Altenkirch, M.F. Bundy, S. Bhattacharjee, L.I.N. Tang, K. Sacksteder, Creeping flame spread along fuel cylinders in forced and natural flows and microgravity, Proc. Combust. Inst. 28 (2000) 2835–2842.

[31] C. Fernandez-Pello, The solid phase, in: G. Cox (Ed.), Combust. Fundam. Fire, Academic Press Limited, 1994: pp. 31–100.

[32] F.A. Williams, Mechanisms of fire spread, Symp. Combust. 16 (1976) 1281–1294. doi:10.1016/S0082-0784(77)80415-3.

[33] J. Quintiere, A simplified theory for generalizing results from a radiant panel rate of flame spread apparatus, Fire Mater. 5 (1981) 52–60. doi:10.1002/fam.810050204.

[34] M.A. Delichatsios, Creeping flame spread: energy balance and application to practical materials, Symp. Combust. 26 (1996) 1495–1503.

[35] J.N. de Ris, Spread of a laminar diffusion flame, Symp. Combust. 12 (1969) 241–252. doi:10.1016/S0082-0784(69)80407-8.

[36] I.S. Wichman, Theory of opposed-flow flame spread, Prog. Energy Combust. Sci. 18 (1992) 553–593. doi:10.1016/0360-1285(92)90039-4.

[37] S. Bhattacharjee, R.A. Altenkirch, N. Srikantaiah, M. Vedhanayagam, A Theoretical Description of Flame Spreading over Solid Combustibles in a Quiescent Environment at Zero Gravity, Combust. Sci. Technol. 69 (1990) 1–15. doi:10.1080/00102209008951599.

[38] T. Hirano, K. Saito, Fire spread phenomena: The role of observation in experiment, Prog. Energy Combust. Sci. 20 (1994) 461–485. doi:10.1016/0360-1285(94)90001-9.